Three-state Potts model and anomalous tricritical points

1973 J. Phys. A: Math. Nucl. Gen. 6 1310

(http://iopscience.iop.org/0301-0015/6/9/007)

J. Phys. A: Math., Nucl. Gen., Vol. 6, September 1973. Printed in Great Britain.

Three-state Potts model and anomalous tricritical points

J P Straley†§ and Michael E Fisher‡

† Department of Physics, Rutgers University, New Brunswick, New Jersey 08903, USA
‡ Baker Laboratory, Cornell University, Ithaca, New York 14850, USA

Received 30 March 1973

Abstract. Thirteen terms are presented of the low-temperature series for the free energy of the three-state Potts model in arbitrary external fields. Extrapolation of the series for specific heat, order parameter, and susceptibilities indicates that the transition in zero field is continuous (in contrast to the Landau prediction) with exponents $\alpha = \alpha' = 0{\cdot}05 \pm 0{\cdot}10$, $\beta = 0{\cdot}10 \pm 0{\cdot}01$, $\gamma' \simeq 1{\cdot}5 \pm 0{\cdot}2$ and $\gamma'_{\perp} = 1{\cdot}1 \pm 0{\cdot}1$. These conclusions suggest the presence of an 'anomalous' tricritical point in the model; the associated phase diagram is discussed and contrasted with the phenomenological predictions.

1. Introduction and summary

Some time ago Potts (1952) proposed a generalization of the standard Ising model in which each site of the lattice can be in one of q distinct states. Nearest-neighbour sites (in the simplest realization of the model) interact with energy ϵ_0 if they are in the *same* state but with energy ϵ_1 if they are in *different* states. In the 'ferromagnetic' case one has $\epsilon_1 > \epsilon_0$. Evidently the standard Ising model corresponds to $q = 2$.

Potts studied the matrix approach and, for the case of the plane square lattice, discovered a duality transformation carrying low temperatures into high temperatures and vice versa. In later but apparently independent work Kihara *et al* (1954) discussed the same model and developed a graphical derivation of the duality relation. Some time ago one of the authors (MEF) derived a more general graphical analysis for an arbitrary planar lattice and more recently Mittag and Stephen (1971) have presented a detailed discussion using both topological and algebraic methods. By assuming, as is true for the Ising case ($q = 2$), that there is only one transition temperature in the absence of external symmetry-breaking fields, Potts located the transition point, T_0, of the square lattice for general q as the fixed point of the duality transformation.

In this work we will discuss the ferromagnetic model on the square lattice, specifically for the case $q = 3$. Let n_k be the fraction of lattice sites in the kth state. In the thermodynamic limit the ordered state of the model is characterized by nonzero expectation for the densities

$$\delta n_k = n_k - q^{-1}, \tag{1}$$

in the limit that appropriate symmetry-breaking fields are reduced to zero. In the case of odd q (in particular, $q = 3$) the δn_k are not symmetrical about zero, in the sense that positive and negative values (when meaningful) describe physically quite distinct configurations. It follows that, if one postulates a formal expansion of the free energy

§ Present address: Department of Physics, University of Kentucky, Lexington, Ky 40506, USA.

near the transition point in powers of the δn_k, one must expect *odd* powers to occur. Thus according to the well known phenomenological argument of Landau (1937) the zero-field phase transition is predicted to be of first order as a function of temperature (see appendix 1). In particular then, the Potts three-state model might be expected to exhibit behaviour similar to the somewhat related Zwanzig (1963) lattice model for liquid crystals. Indeed the usual mean field approximations, when applied to the $q = 3$ Potts model, do indicate such a discontinuous first order transition. The analysis is sketched in appendix 1.

The Landau theory is, however, by no means unassailable. Even granting the possibility of the postulated Taylor series for the free energy (on which the method relies), the argument can fail if the cubic term 'accidentally' vanishes at the transition point. This might occur due to the intervention of some special, perhaps unsuspected or 'hidden' symmetry of the model. More generally we know that Taylor series expansions of the free energy about a transition point do *not* exist for most realistic symmetric models (Fisher 1967, Kadanoff *et al* 1967), where the Landau theory always predicts a second order transition with classical exponents. There seem to be no good grounds for accepting a Taylor expansion in more general cases.

In fact we strongly suspect that the Landau prediction *does* fail for the three-state Potts model on the square lattice. The appropriate exact series expansions, and their analysis which we report below, do not really support the expectation of a first order transition. On the contrary they can be consistently interpreted as describing a continuous (or higher order) phase transition characterized by well defined critical point exponents $\alpha = \alpha'$, β, and γ'. The estimated values of these exponents, $\alpha \simeq 0{\cdot}05$, $\beta \simeq 0{\cdot}10$, $\gamma' = 1{\cdot}5 \pm 0{\cdot}2$, do not indeed differ greatly from those for the square lattice Ising model. In addition, an exponent $\gamma'_\perp$ is introduced to describe the transverse fluctuations (eg of $(n_2 - n_1)$ in a 3-rich phase), which also appear to diverge strongly at the zero-field transition point ($\gamma'_\perp \simeq 1{\cdot}1$).

It is illuminating to consider the consequences of this conclusion for the form of the full phase diagram of the model. To this end we introduce (for $q = 3$) three external fields ζ_k ($k = 1, 2, 3$) which couple to the distinct states by adding a term

$$-N(\zeta_1 n_1 + \zeta_2 n_2 + \zeta_3 n_3) \tag{2}$$

to the total energy expression for an N-site lattice. Since the model is clearly restricted by $n_1 + n_2 + n_3 = 1$, only the differences say, $\zeta_1 - \zeta_3$ and $\zeta_2 - \zeta_3$ are relevant to the thermodynamic properties. We may thus take $\zeta_3 = 0$. On the other hand symmetry is preserved if one retains all these fields but imposes the relation

$$\zeta_1 + \zeta_2 + \zeta_3 = 0. \tag{3}$$

This in turn leads to a 'triangle diagram' for representing the phase space, $(\zeta_1, \zeta_2, \zeta_3; T)$, of the model.

Then, according to Landau theory or the mean field approximation, the transition point in zero field actually represents a *quadruple point* where four phases, namely 1-rich, 2-rich, 3-rich and disordered can coexist, as illustrated in figure 1. The quadruple point (marked q in the figure) is the meet of four *triple point lines* (marked 0, 1, 2, 3) and six *coexistence surfaces* on each of which two phases, for example 1-rich and 2-rich, or 2-rich and disordered, etc, can coexist. No abnormally large or 'critical' fluctuations in any variable would be expected in any of the phases in the vicinity of such a quadruple point.

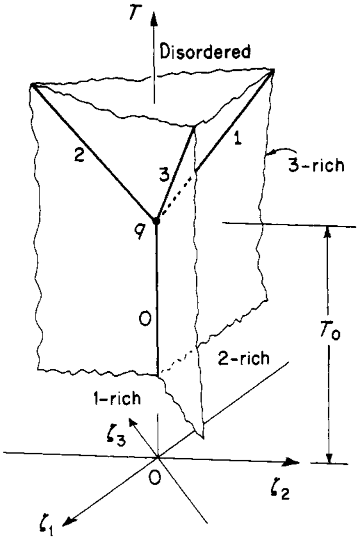

Figure 1. Phase diagram of the three-state Potts model near zero fields according to the phenomenological Landau theory. The transition in zero field is a quadruple point marked q, at the meet of four triple point lines labelled 0, 1, 2, and 3. Two of the four phases coexist on each surface.

Conversely, the critical behaviour, which the evidence suggests characterizes the zero-field transition, rather indicates that the full phase diagram might be as sketched in figure 2. In this case the transition point in zero field is a *tricritical point* (marked t) formed by the join of three critical lines. Each line corresponds, in fact, to a $q = 2$ or Ising-like transition between the phases: (1-rich : 2-rich), (2-rich : 3-rich), and (3-rich : 1-rich). The more detailed arguments for this conclusion will be presented in § 5. It is noteworthy, however, that a tricritical point such as this differs significantly from the tricritical points expected in other systems (Griffiths 1970, 1973). A typical or 'normal' tricritical point (depending on two fields ζ and ζ') is illustrated in figure 3. By contrast with the 'anomalous' situation in figure 2, we note that one of the three critical lines is distinguished from the other two, which, in turn, bound two 'wing-like' coexistence surfaces w_+ and w_-. In particular, the distinguished or dominant critical line meets the other two lines tangentially and then 'splits'. Thus one cannot draw a plane through the tricritical point so that all critical lines lie on one side (and are not tangent to it). Such a plane can clearly be drawn through the anomalous tricritical point in figure 2. Among reasons for terming the Potts model tricritical point (if it really exists) 'anomalous' are, firstly, that such an arrangement of the critical lines cannot be produced naturally, in the phenomenological theory. Secondly that the composition triangle in the tricritical region necessarily exhibits unusual features, which will be explained below.

Whether such anomalous tricritical points can or do exist in real physical systems remains to be seen. At the present time, indeed, only few normal tricritical points have been subjected to detailed experimental investigation. In any event, our analysis suggests that such transitions might occur in systems with threefold or close-to-threefold symmetry.

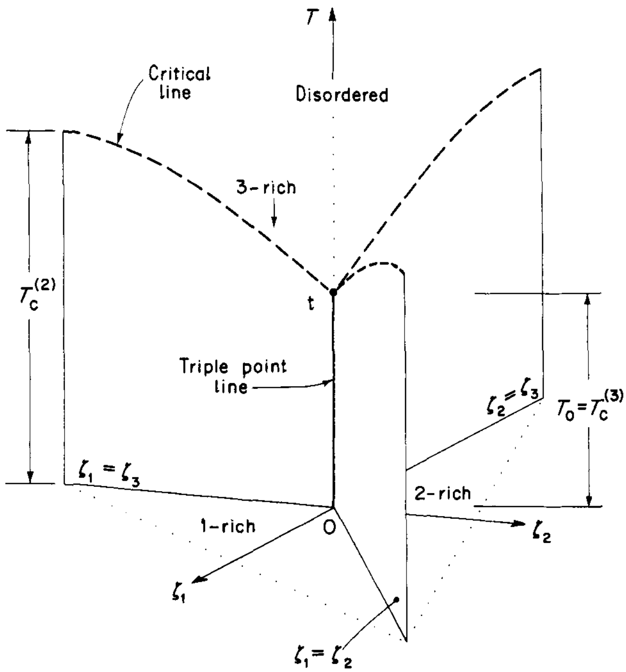

Figure 2. Phase diagram for the three-state Potts model indicated by the conclusion that the zero-field transition at T_0 is a critical point, in fact, an 'anomalous' tricritical point. The limit $\zeta_3 \to -\infty$ yields a two-state or Ising model with critical temperature $T_c^{(2)}$ and, similarly, for ζ_2 or $\zeta_1 \to -\infty$.

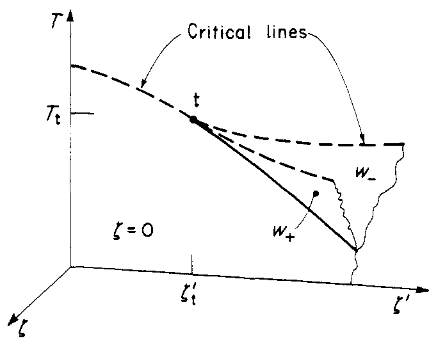

Figure 3. Appearance of a 'normal' tricritical point, labelled t, of the type discussed in Griffiths (1970, 1973). Here ζ denotes the dominant ordering field while w_+ and w_- label the 'wings' arising when the secondary field ζ' is increased beyond its tricritical value ζ'_t.

2. Low temperature expansions

If N_{kl} denotes the number of bonds in a configuration of the model which join a site in state k to one in state l, then the total energy for a lattice of N sites can be written

$$E = \epsilon_1(N_{12} + N_{23} + N_{31}) - \zeta_1 N n_1 - \zeta_2 N n_2, \tag{4}$$

where we have exercised the freedom to set $\zeta_3 = 0$ and have, with no loss of generality, taken $\epsilon_0 = 0$. If we suppose $\zeta_1, \zeta_2 < 0$, almost all sites will be in state 3 at low temperatures. Then an expansion of the partition function in powers of

$$x = \exp\left(\frac{-\epsilon_1}{kT}\right), \qquad y_1 = \exp\left(\frac{\zeta_1}{kT}\right), \qquad y_2 = \exp\left(\frac{\zeta_2}{kT}\right)$$

may be obtained by considering configurations in which, successively, 0, 1, 2, 3, ... sites are in the minority states 2 or 3. Thus one finds

$$Z_N = 1+N(y_1+y_2)x^4+2N(y_1^2+y_2^2)x^6+4Ny_1y_2x^7+\ldots. \tag{5}$$

In the zero-field case ($y_1 = y_2 = 1$) the expansion has been carried to order x^{16} for general q by Kihara *et al* (1954).

A general term of the expression of the partition function can be directly related to a set of graphs, which directly represent some configuration of minority sites. A typical graph is some polygon or group of disjoint polygons, possibly containing interior partitions separating regions of different types of minority sites. If the total perimeter of the graph is l, and the cluster contains m_1 1-sites and m_2 2-sites, then the graph is a contribution to the term $x^l y_1^{m_1} y_2^{m_2}$. We have constructed a list of all polygons of perimeter 13 or less, which gives all terms of third order in y_1 and y_2, as well as some contributions from the more compact configurations of four, five,... minority sites. To generate the expansion of the partition function it is also necessary to calculate the number of ways each configuration can occur on the lattice.

The expansion was generated for general q and zero field, as well as general fields for $q = 3$. The former series agrees with that of Kihara *et al.* Similarly, when y_2 (or y_1) vanishes the latter expansion reduces to the known (Domb 1960) $q = 2$ (standard Ising) model expressions.

The analysis to be presented below is restricted to $q = 3$, despite the fact that equivalent series for higher q are readily generated. It seems quite possible that a short series cannot be used to discuss large q, since the beginning terms of the series do not contain full information about the problem being discussed. For example, the first three terms of equation (5) describe a pair of independent Ising models, and only in the last term do the interactions between the minority sites play a role.

From the series for the partition function one readily derives an expansion for the limiting free energy per site, namely,

$$F(\zeta_1, \zeta_2, T) = -kT \lim_{N\to\infty} N^{-1} \ln Z_N(\zeta_1, \zeta_2, T). \tag{6}$$

This expansion is presented in appendix 2. By differentiation with respect to x (or T) series for the internal energy and specific heat are obtained. These series are listed in appendix 2 for the limit of zero field (where the results follow directly from Kihara *et al*).

Recalling that for $\zeta_1, \zeta_2 < 0$ the system will be in the 3-rich phase, we define the spontaneous order parameter by

$$\begin{aligned}\Psi_0(T) &= \lim_{\zeta_1,\zeta_2\to 0^-} \left(\tfrac{3}{2}\langle n_3\rangle - \tfrac{1}{2}\right)\\ &= 1-\tfrac{3}{2}(\langle n_1\rangle_0+\langle n_2\rangle_0)\\ &= 1+\frac{3}{2}\left[\frac{\partial F}{\partial \zeta_1}+\frac{\partial F}{\partial \zeta_2}\right]_{\zeta_1=\zeta_2=0^-}.\end{aligned} \tag{7}$$

The normalization has been chosen so that $\Psi_0(0) = 1$. The series expansion for $\Psi_0(T)$ follows directly from that for F and is again tabulated in appendix 2.

It is also fruitful to define two susceptibilities. The first of these, the longitudinal or parallel susceptibility is defined by

$$\chi = \frac{2}{3}\frac{\partial\Psi}{\partial\zeta_3} = -\left(\frac{\partial}{\partial\zeta_1}+\frac{\partial}{\partial\zeta_2}\right)(\langle n_1\rangle+\langle n_2\rangle) = -\left(\frac{\partial}{\partial\zeta_1}+\frac{\partial}{\partial\zeta_2}\right)^2 F. \tag{8}$$

On the line of symmetry $\zeta_1 = \zeta_2$ (implying $\langle n_1\rangle = \langle n_2\rangle$) this is analogous to the standard susceptibility of, for example, a ferromagnet; it measures the response of the order parameter to the field favouring ordering and is proportional to the fluctuations of the order parameter. In addition we define a transverse or perpendicular susceptibility

$$\chi_\perp = \left(\frac{\partial}{\partial\zeta_1}-\frac{\partial}{\partial\zeta_2}\right)(\langle n_1\rangle-\langle n_2\rangle) = -\left(\frac{\partial}{\partial\zeta_1}-\frac{\partial}{\partial\zeta_2}\right)^2 F, \tag{9}$$

which measures the ease with which one can alter the ratio of n_1 to n_2 in the 3-rich phase (holding n_3 constant). The series for χ and $\chi_\perp$ in the zero-field limit $\zeta_1 = \zeta_2 \to 0^-$ are included in appendix 2.

3. Dual transformation

Since the square lattice is self-dual the dual transformation provides an equation for the zero-field free energy which relates its value at a (say, low) temperature T to that at a dual (then, high) temperature T^*. From Potts (1952) we find for the case $q = 3$,

$$\frac{F(T)}{kT} = \ln\tfrac{1}{3}(1+2x)^2+\frac{F(T^*)}{kT^*}, \tag{10}$$

where

$$x(T) = \exp\left(-\frac{\epsilon_1}{kT}\right) = \frac{1-x(T^*)}{1+2x(T^*)} = v(T^*). \tag{11}$$

These equations relate the high and low temperature expansions of the zero-field free energy, energy, and specific heat. In addition they can be used to generate approximate high temperature expressions from approximate low temperature expressions based, for example, on a summation of a subset of graphs. If there is a single transition point in zero field it must occur at a self-dual temperature, T_0, such that $x(T_0) = v(T_0)$. This gives

$$x_0 = x(T_0) = \tfrac{1}{2}(\sqrt{3}-1) = 0{\cdot}366025\ldots. \tag{12}$$

We use the subscript 'zero' rather than 'c' in order to stress that *a priori* we do not know the character of this transition, that is, whether it is first order or continuous. The dual transformation does not yield that information. However, if the transition is continuous it follows (Kihara *et al* 1954) that the critical value of the energy per site is

$$\epsilon_1^{-1}U_c = (1-\sqrt{\tfrac{1}{3}}) = 0{\cdot}42264\ldots. \tag{13}$$

Furthermore if the specific heat diverges at the transition the singularity must be symmetric, that is, we must have $\alpha' = \alpha$ or $C \sim |x-x_0|^{-\alpha}$ as $x \to x_0\pm$.

The duality relation does not apply directly to the order parameter or the susceptibilities and correlations, although, as in the Ising case (Fisher and Ferdinand 1967, Fisher 1969), certain zero-field information concerning the correlation function does undergo transformations. We have not, however, explored or exploited such relations.

4. Series analysis

Owing to the relative shortness of our series as a function of the field variables (ie complete only to third order in y_1 and y_2) we have confined the present analysis to the zero field series. It would, however, be very interesting to obtain and study longer expansions in powers of y_1 and y_2 in order to confirm the full field dependence and to estimate the exponent δ, etc.

The analysis we present is based entirely on the behaviour of the Padé approximants to various series. Ratio techniques did not seem to be useful on account of the irregularity of the series.

4.1. Energy and specific heat

In the case of a continuous transition the internal energy $U(T)$ is continuous but is expected to have a divergent derivative at the transition point T_0 (which is then a 'critical' point). Neither a truncated series expansion nor a direct Padé approximant can represent such behaviour properly and so they will not be considered.

Direct Padé approximants to the specific heat† yield poles in the vicinity of $x = 0{\cdot}38$ which is only a few per cent larger than the transition point value $x_0 = 0{\cdot}366$. Series for the logarithmic derivative, $(\mathrm{d}/\mathrm{d}x) \ln (C(x)$, exhibit poles in a similar region with residues of about 0·6. This behaviour could be interpreted as indicating a first order transition, since if $C \sim |x-x_1|^{-0\cdot6}$ with $x_1 > x_0$, the specific heat would be bounded in the transition region x_0. The internal energy, calculated say by integrating $C(x)$, will then undoubtedly be discontinuous through x_0. Previous experience, and the study of model functions, suggests however, that such behaviour could also be consistent with a weaker singularity (α close to zero) at the transition point itself. In that case the previous analysis is inadequate. Consequently, the series for $\mathrm{d}C/\mathrm{d}x$ was constructed and Padé analysed. Figure 4 shows how the poles of direct approximants to the series and to its logarithmic derivatives are distributed. Note that in many cases the poles of the approximants lie *below* x_0 which, via duality, would imply two singularities as a function of T. We feel such a possibility can be safely discounted. Accordingly the analysis suggests that the specific heat diverges *at* x_0 with a close-to-logarithmic singularity. Clearly the available precision of an estimate of the exponent α is not great, but, bearing in mind the trends of the residue–pole relation we conclude

$$\alpha = \alpha' = 0{\cdot}05 \pm 0{\cdot}10. \tag{14}$$

Since the singularity is in any case quite close to logarithmic we have constructed approximants for the specific heat by integrating the [4/4] and [5/6] direct Padé approximants to $\mathrm{d}C/\mathrm{d}x$. The approximations for $C(x)$ have logarithmic singularities at the poles of the parent approximant which, for these choices, are very close to x_0 (eg the

† Here and below, references to the specific heat actually refer to the series expansion (in x) of the function $kT^2\epsilon_1^{-2}C$.

[5/6] approximant has a pole at $x = 0{\cdot}366007$). Figure 5 compares the 'integrated [5/6]' approximation with the truncated series itself and with a direct Padé approximant to it. The dual transformation yields the appropriate high-temperature branch of the plot.

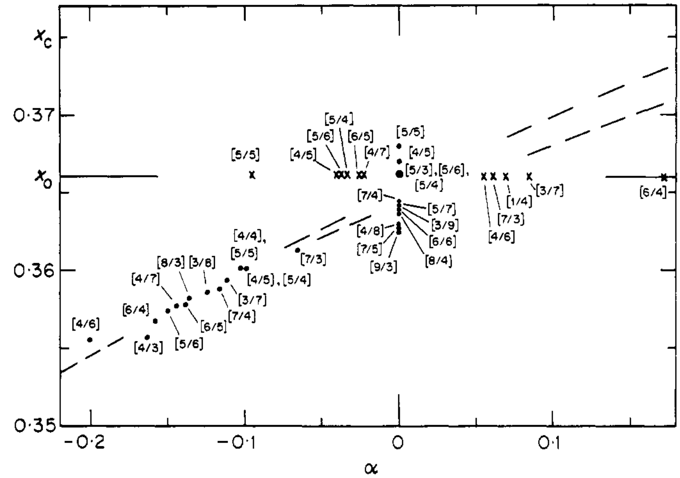

Figure 4. Summary of the analysis of the specific heat series. Shown are (*a*) the poles of Padé approximants to $(d/dx)\ln(dC/dx)$ and corresponding residues interpreted as estimates for the exponent α; (*b*) the poles of approximants to (dC/dx), on the line $\alpha = 0$; and (*c*) the value at x_0 of approximants to the exponent function $\alpha^*(x) = (x_0 - x)(d/dx)\ln(dC/dx) - 1$, on the line $x = x_0$. The broken lines suggest the general trend of the $\alpha^*(x)$ relation.

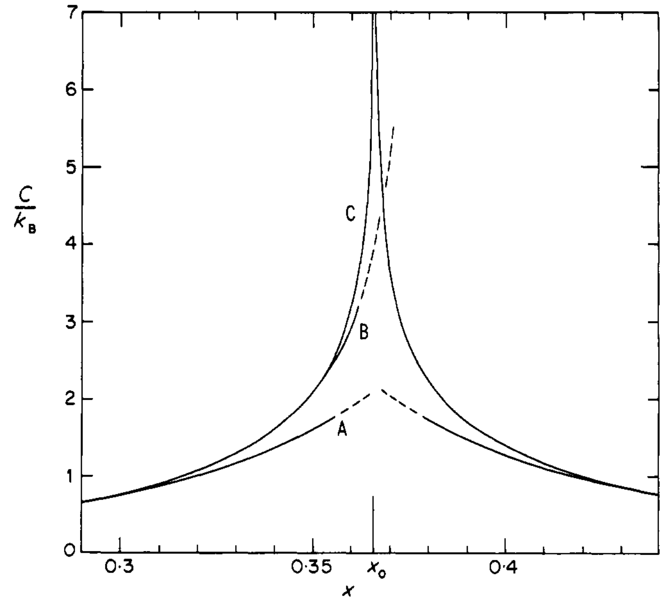

Figure 5. Approximations and estimates for the specific heat; curve A the truncated series for C; curve B direct approximant to the series for C; curve C integral of the [5/6] approximant to the series for (dC/dx) together with the complementary high temperature branch furnished by the dual transformation. Note the comparatively narrow range of the variable x relative to figure 6.

Now we may return to the question of the continuity of the internal energy. The logarithmic approximations to the specific heat $C(x)$ were integrated numerically yielding the estimated behaviour of the internal energy displayed in figure 6. The dual transformation again provides the high-temperature branch. The approximation for $U(T)$ is evidently almost continuous at x_0; the apparent discontinuity is $\Delta U \simeq 0{\cdot}04 U_{\mathrm{max}}$. If we had calculated the approximation for $U(T)$ on the assumption of a higher value of α, such as our central estimate 0·05, the magnitude of this numerical discontinuity would be further reduced. In view of the uncertainties in α, however, it does not seem worthwhile at this stage to undertake more elaborate extrapolations. The evidence clearly suggests that $U(T)$ is, in fact, continuous at T_0 so that the three-component Potts model exhibits a continuous transition, or genuine critical point, with a specific heat which diverges weakly but, probably, somewhat more strongly than logarithmically.

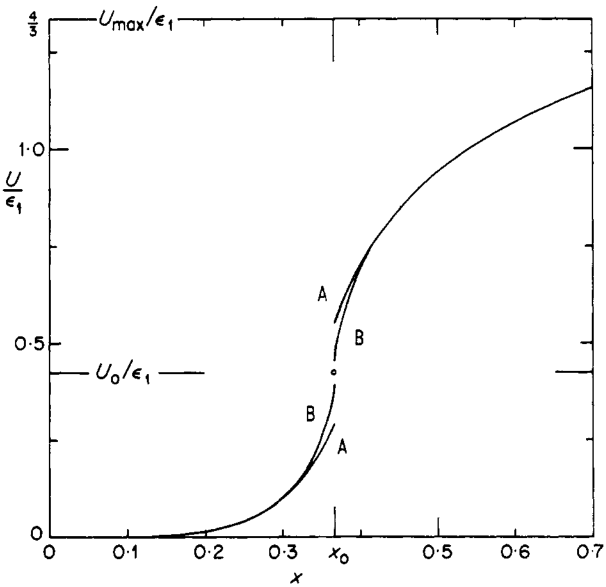

Figure 6. Approximations for the internal energy: curve A the truncated series for U and its dual; curve **B** the double integral of the [5/6] Padé approximant to $(\mathrm{d}C/\mathrm{d}x)$ used for curve C in figure 5, and the dual extension. Note the critical value of U fixed by duality for a continuous transition.

4.2. Spontaneous order

The truncated series for the zero-field or spontaneous order parameter $\Psi_0(T)$, defined in (7), has its first real positive zero at $x = 0{\cdot}47$ which lies appreciably far beyond the transition point $x_0 \simeq 0{\cdot}366$. The value of the truncated series at x_0 is 0·856. However, even the direct Padé approximants to the series yield the lower transition point value of $\Psi_0(T) \simeq 0{\cdot}81$ and closer zeros at $x \simeq 0{\cdot}41$. Each of these approximants has a pole very slightly beyond the zero at $x = 0{\cdot}42 \pm 0{\cdot}01$; such behaviour is often symptomatic of a nonanalytic zero lying closer to the origin. Accordingly it is appropriate to analyse the logarithmic derivative $(\mathrm{d}/\mathrm{d}x) \ln \Psi_0(x)$. As is evident from table 1 all the higher order approximants exhibit poles in the range 0·363 to 0·366 with residues of 0·10 to 0·11. Discounting again the possibility of a transition lying below T_0 this is strong evidence

Table 1. Analysis of order parameter series

Padé approximants to $(d/dx)\ln\Psi_0$			Value at x_0 of approximants to $(x_0-x)(d/dx)\ln\Psi_0$	
Approximant	Pole	Residue	Approximant	Value
[8/4]	0·3645	0·1014	[10/3]	0·1084
[7/5]	0·3635	0·0990	[9/4]	0·1055
[6/6]	0·3635	0·0990	[8/5]	0·1332†
[5/7]	0·3649	0·1027	[7/6]	0·1402†
[4/8]	0·3645	0·1016	[6/7]	0·1059
[7/4]	0·3635	0·0992		
[6/5]	0·3636	0·0992	[8/4]	0·1067
[5/6]	0·3636	0·0992	[7/5]	0·1014
[4/7]	0·3657	0·1048		
[5/5]	0·3635	0·0990		

† These approximants have a paired pole and zero near x_0, and probably should be ignored.

that $\Psi_0(T)$ vanishes continuously at T_0 as at a normal critical point. Granting this, estimates for the exponent β may be found by evaluating approximants to the series for

$$\beta^*(x) = (x-x_0)\frac{d}{dx}\ln\Psi_0(x) \tag{15}$$

at $x = x_0$. These values lie between 0·100 and 0·106 for the higher order approximants.

As a further check on the conclusion that $\Psi_0(T)$ vanishes like $(x-x_0)^\beta$ with $\beta \simeq 0{\cdot}1$ the series for Ψ_0^8, Ψ_0^9, and Ψ_0^{10} were constructed. Direct approximants to these series have simple zeros concentrated in the ranges $x = 0{\cdot}369$ to $0{\cdot}383$, $0{\cdot}366$ to $0{\cdot}370$ and, with somewhat more scatter, $0{\cdot}364$ to $0{\cdot}368$, respectively. These results support the estimate

$$\beta = 0{\cdot}103 \pm 0{\cdot}010. \tag{16}$$

Although the confidence limits could be over optimistic, the present evidence is not really consistent with the exponent value $\beta = \frac{1}{8}$, which applies to the standard ($q = 2$) Ising model. In view of the fundamentally different symmetry properties of the three-state model, this is hardly surprising. On the other hand, the low value of β (relative to typical experimental values around $\frac{1}{3}$) undoubtedly reflects as expected, the two-dimensional character of the model.

In summary the analysis of the order parameter expansions indicates strongly that the transition of the model is continuous with a well defined exponent β close to $\frac{1}{10}$ and very probably less than $\frac{1}{8}$.

4.3. Susceptibilities

The series for the susceptibilities seem to be less regularly behaved than those for C and Ψ_0. Poles of the approximants to the logarithmic derivatives of χ and $\chi_\perp$ lie in the range 0·32 to 0·37, suggesting again that the singularity is located at x_0. Evaluation of the approximants to the exponent functions $\gamma'^*(x)$ and $\gamma'^*_\perp(x)$, defined in analogy to (13), yield the estimates exhibited in table 2. From these one might conclude

$$\gamma' = 1{\cdot}5 \pm 0{\cdot}1, \qquad \gamma'_\perp = 1{\cdot}10 \pm 0{\cdot}05. \tag{17}$$

Table 2. Analysis of the susceptibility series

Padé approximants to $(d/dx)\ln(x^{-4}kT\chi)$			Value at x_0 of approximants to $(x-x_0)(d/dx)\ln(x^{-4}kT\chi)$	
Approximant	Pole	Residue	Approximant	Value
[5/3]	0·3788	−1·882	[5/4]	−1·492
[4/4]	0·3609	−1·387	[4/5]	−1·331
[3/5]	0·3654	−1·503	[5/3]	−1·485
[3/4]	0·3534	−1·252	[4/4]	−1·485
[4/3]	0·3212	−0·785	[3/5]	−1·695
[3/3]	0·2995	−0·562	[4/3]	−1·486
Padé approximants to $(d/dx)\ln(x^{-4}kT\chi_\perp)$			Value at x_0 of approximants to $(x-x_0)(d/dx)\ln(x^{-4}kT\chi_\perp)$	
Approximant	Pole	Residue	Approximant	Value
[5/3]	0·3609	−1·002	[5/4]	−1·094
[4/4]	0·3639	−1·060	[4/5]	−1·095
[3/5]	0·3639	−1·060	[5/3]	−1·110
[4/3]	0·3733	−1·208	[4/4]	−1·086
[3/4]	0·3638	−1·509	[3/5]	−1·101
[3/3]	0·3712	−1·175	[4/3]	−1·093

However, the confidence limits here are probably subject to significant modification since the series are relatively short and, as mentioned, somewhat irregular.

A check on these exponent estimates can be obtained by means of the Rushbrooke inequality (Rushbrooke 1963)

$$\alpha' + 2\beta + \gamma' \geqslant 2. \tag{18}$$

This can be proved on the basis of the convexity of the free energy (Fisher 1967); in the present case the necessary convexity is easily established for $\zeta_1 = \zeta_2 \leqslant 0$. According to the estimates (14), (16) and (17) the left hand side of (18) totals only $1·76 \pm 0·21 \leqslant 1·97$. A similar difficulty was noted by Essam and Fisher (1963) in their analysis of the low temperature susceptibilities of the plane $q = 2$ Ising lattices. The shorter series, particularly, on the honeycomb and square lattice, yielded estimates of γ' lying 0·1 to 0·2 below the rigorous lower bound $\gamma' = 1·75$. Accordingly we believe that the estimates (17) for γ' and $\gamma'_\perp$ might be too low by a similar amount. Realistically, then, the confidence limits in (17) should probably be doubled in size.

5. Nature of the phase diagram

Our analysis of the zero-field series of the three-state Potts model has indicated rather strongly that the transition is continuous. If this is correct, it has some rather striking implications for the shape of the phase diagram in the full $(\zeta_1, \zeta_2, \zeta_3; T)$ space (where the restriction (3) will now be utilized in order to preserve the symmetry).

To understand the phase diagram let us first suppose that one field, say ζ_3, is large and negative. Then very few sites will be in state 3. Consequently the system will behave like a two-state or standard Ising model, with a few 'impurities', that is, sites in state 3.

Accordingly one expects to find, in this region of phase space, a planar *coexistence surface*, $\zeta_1 = \zeta_2$, bounded by a line of critical points. As $\zeta_3 \to -\infty$ the temperature on this line will approach $T_c^{(2)}$, the critical temperature of the square lattice Ising model. By symmetry, the situation for large negative ζ_2 and ζ_3 must be similar. Thus the appearance of the phase space will be as indicated in figure 7, where portions of the three coexistence surfaces and their critical lines are shown.

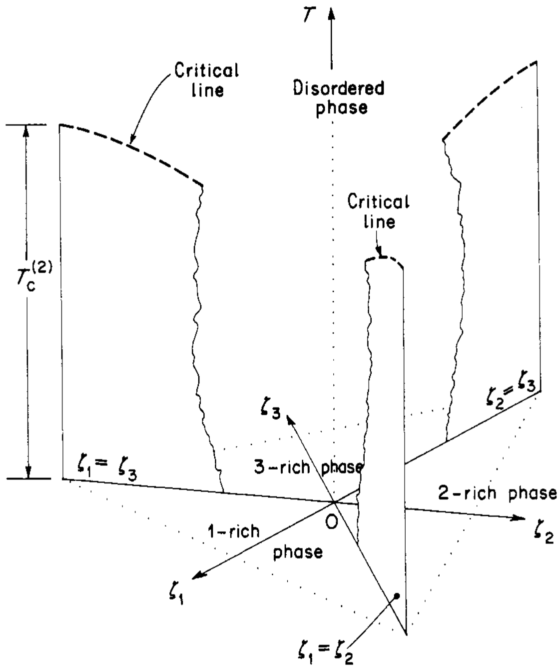

Figure 7. Full phase diagram for the three-state model showing the behaviour that follows by considering the Ising-like limits ζ_1, or ζ_2, or $\zeta_3 \to -\infty$.

In order to complete the central region of the diagram we note that at low temperatures, the three distinct phases, 1-rich, 2-rich, and 3-rich, respectively, can coexist only at the point of symmetry $\zeta_1 = \zeta_2 = \zeta_3 = 0$. Thus at all temperatures below the symmetric transition point T_0 the three coexistence surfaces must continue until they meet in a triple point line; this is shown as a bold line in figure 2. Finally, if the zero-field transition is critical, in the sense of having divergent fluctuations, it is natural to expect that it lies *on* the continuation of the three critical lines originating at the Ising model limits. The whole situation should thus be as illustrated in figure 2. Evidently the transition at $T_0 = T_c^{(3)}$ is a tricritical point; but, as observed in the introduction, its character is quite distinct from that of the tricritical points normally considered. (Compare again with the normal tricritical point illustrated in figure 3.)

It is instructive to draw the composition diagrams at various temperatures corresponding to this tricritical phase diagram. Figure 8 shows sample composition triangles: as usual the pure phases correspond to the appropriately labelled corners; the tie lines on the diagrams indicate the two-phase regions; the black dots denote the associated

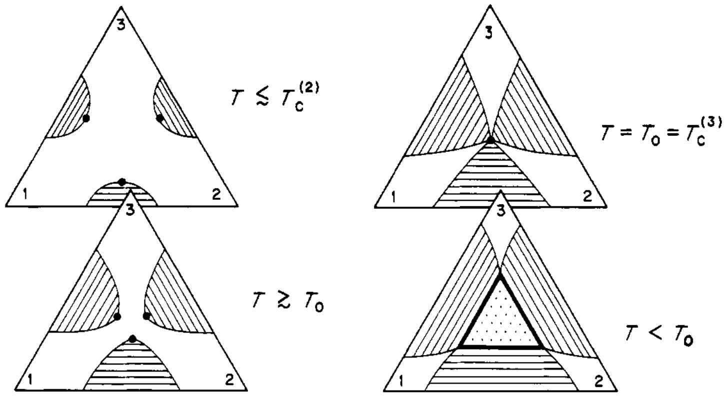

Figure 8. Composition diagrams for selected temperatures corresponding to the full phase diagram of figure 2. An anomalous tricritical point occurs at $n_1 = n_2 = n_3$ when $T = T_0 = T_c^{(3)}$. The tie lines reveal the two-phase regions; the stippling denotes a three-phase region.

critical points (or plait points). In the low temperature diagram ($T < T_0$) the three-phase region, corresponding to $\zeta_1 = \zeta_2 = \zeta_3 = 0$, is marked by stippling; any mixture with a composition lying in this triangle, will break up into domains of the three phases corresponding to the corners of the triangle. A somewhat unusual feature of the diagram is the three pointed coexistence curves which arise just at the tricritical transition point $T = T_0 = T_c^{(3)}$; correspondingly as $T \to T_0+$, the coexistence curves will become increasingly pointed.

As noted in the introduction, the phenomenological theory and the mean field approximations predict that the transition at T_0 is a *quadruple point q* at which an equicomposition or disordered phase, coexists with three asymmetric phases each rich in one of the three states. The corresponding local region of the phase diagram was illustrated in figure 1. The associated behaviour of the full phase diagram is sketched in figure 9. Evidently the three web-like surfaces w_1, w_2, and w_3, which now join the original coexistence surfaces $\zeta_1 = \zeta_2, \zeta_2 = \zeta_3$, and $\zeta_1 = \zeta_2$, extend to form the 'wings' of three new tricritical points (labelled t_1, t_2, and t_3). These three tricritical points are, however, of the orthodox type shown in figure 3.

The composition diagrams for $T_0 \leqslant T < T_c^{(2)}$ now exhibit appreciably more complicated behaviour as evident in figure 10. A special role is played not only by the tricritical temperature T_t (equal, by symmetry for t_1, t_2 and t_3) but also by the otherwise undistinguished temperature, T_m, which is the minimum critical temperature. This corresponds to the lowest points on the web surfaces w_1, w_2 and w_3 in figure 9. In the interval $T_0 < T < T_t$ four distinct phases appear in the composition triangle; however, no more than three of these can coexist at the same time. (The three-phase regions are again stippled.) Below T_0 and in the region near and above $T_c^{(2)}$, the composition diagrams have the same character as before. The full sequence of composition diagrams for the phenomenological theory can thus be obtained by replacing the two triangles in figure 8 labelled $T \gtrsim T_0$ and $T = T_0 = T_c^{(3)}$, by the sequence of four in figure 10.

Although, to our knowledge, there are no real systems displaying composition diagrams with the full symmetry of figure 10, three-component fluid systems do exist (Roozeboom 1913) which show a number of the topological features displayed—in particular the merging of coexistence curves at a minimum critical point and the existence of enclosed three-phase regions. It would be interesting to try to mimic the three-state Potts model more closely in the laboratory to see which type of phase diagram would be realized.

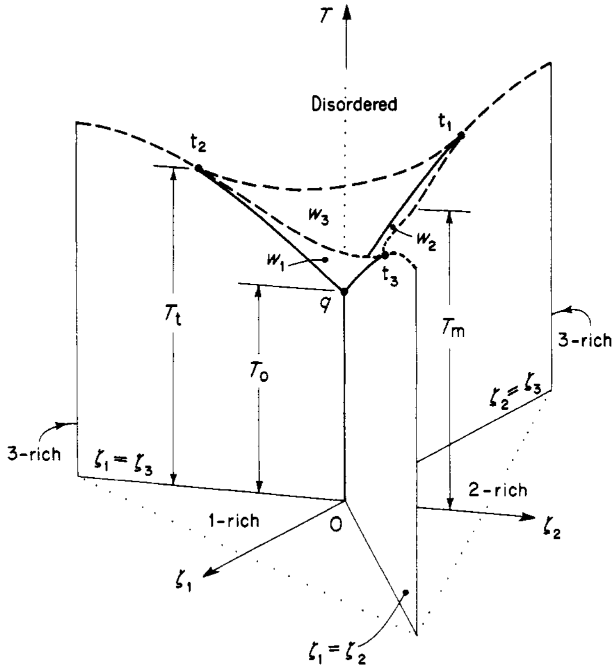

Figure 9. Full phase diagram for the three-state model following from the phenomenological and mean field theories (compare with figure 1). The three tricritical points are labelled t_1, t_2 and t_3; the zero-field transition is the quadruple point labelled q; the lowest critical points occur on the boundaries of the 'webs' or 'wings' w_1, w_2, and w_3, at a temperature T_m.

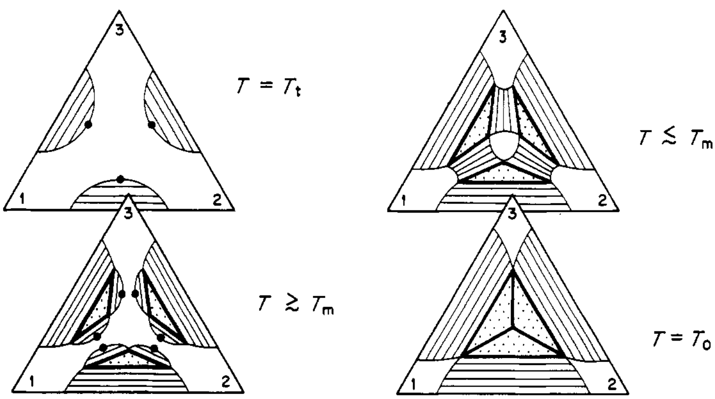

Figure 10. Composition diagrams for various temperatures in the range $T_0 \leqslant T \leqslant T_t$ for the phenomenological phase diagram of figure 9. Tie lines indicate the two-phase regions while stippling denotes the three-phase regions.

Acknowledgments

We would like to thank Franz J Wegner for a helpful comment, and Michael J Stephen for pointing out the paper of Kihara *et al.*

The support of the National Science Foundation partly through the Materials Science Center at Cornell University and partly through grant NSF-GP29516 is gratefully acknowledged.

Appendix 1. Classical theory of the three-state Potts model

Following Landau (1937) we expand the canonical free energy $A(n_1, n_2, n_3, T)$ about the symmetry axis $n_1 = n_2 = n_3 = \frac{1}{3}$. Accordingly we introduce the deviations

$$m_k = n_k - \tfrac{1}{3}, \qquad k = 1, 2, 3 \tag{A.1}$$

which are subject to

$$m_1 + m_2 + m_3 = 0. \tag{A.2}$$

In view of the symmetry of A under all interchanges, $m_j \leftrightarrow m_k$ and the condition (A.2), the expansion to fourth order must have the form

$$A = A_0(T) + r\sum m_k^2 + v m_1 m_2 m_3 + u\left(\sum m_k^2\right)^2 + \dots \tag{A.3}$$

Thus other cubic terms, such as $\Sigma_{j \neq k} m_j^2 m_k$, are simply proportional to $m_1 m_2 m_3$. As usual the coefficients r, v, and u are presumed to vary analytically with T. It is now evident that if $v = 0$, the free energy expression has rotational symmetry and would be appropriate, say, for describing an XY or 'planar' ferromagnet. As r passes through zero a classical second-order transition occurs. Thus to describe the threefold symmetry of the Potts model one must either have $v \neq 0$ or else sixth-order and higher terms must play a crucial role in the expansion. We will take $v > 0$ with no loss of generality.

To analyse (A.3) it is convenient to put

$$M = \tfrac{1}{2}\sqrt{3} m_1, \qquad Q = \tfrac{1}{2}(m_2 - m_3), \qquad v' = 2 \times 3^{-3/2} v, \tag{A.4}$$

which lead to

$$A = A_0 + r(M^2 + Q^2) - v' M (M^2 - 3Q^2) + u(M^2 + Q^2)^2 + \dots \tag{A.5}$$

in which M and Q are independent orthogonal variables. When $r = 0$ it is easy to see that A has three symmetrically placed minima lying on the lines $M = 0, \pm\sqrt{3}Q$. For negative r these minima merely increase in depth and move further out from the origin. The composition triangle, found by taking the convex envelope or double tangents, of the A surface is clearly of the form indicated in figure 8 for $T < T_0$.

As r becomes positive, a metastable minimum appears at the origin $M = Q = 0$. The locations of the three remaining minima may, by symmetry, be found from the equation for A with $Q = 0$. One finds the minima exist provided $r < r_1 = 9v'^2/32u$ and that they always lie further than $M = 3v'/8u$ from the origin. However, for $r = r_0 = v'^2/4u < r_1$, these minima become higher than the one at the origin. Accordingly in zero field for $r > r_0$ the stable state shifts discontinuously to $M = Q = 0$ or $m_k = 0$, $r_k = \frac{1}{3}$ (all k). This identifies the transition at $r(T_0) = r_0$ as a quadruple point where a first order jump of magnitude $\Delta M = v'^2/2u$ occurs from a disordered state to one of the three symmetric k-rich states.

The behaviour away from the centre of the composition triangle now follows by considerations of continuity, and by plotting the contours of constant A in the (M, Q) plane and using the double tangent construction. For example the minimum critical points occur at $M_{\rm m} = v'/4u$ when $r(T_{\rm m}) = r_{\rm m} = 3v'^2/8u$. In this way the form of figures 9 and 10 may be elucidated.

Appendix 2. Free energy series for general q

There are $q-1$ different minority species, and $q-1$ corresponding independent fields. The free energy series is a symmetric function of the $q-1$ variables y_i. The series is given here in an unsymmetrized form, with the convention that each term represents all the terms that can be generated from it by assignment of the subscripts. The subscripts have been suppressed. Thus y^n means $y_1^n + y_2^n + \ldots + y_{q-1}^n$, and (for $q = 4$) yy becomes $y_1y_2 + y_1y_3 + y_2y_1 + y_2y_3 + y_3y_1 + y_3y_2$, with each product represented twice. Then the low-temperature expansion for the free energy is

$$
\begin{aligned}
-\frac{1}{kT}&F(\zeta_1, \zeta_2, \ldots; T)\\
&= yx^4 + 2y^2x^6 + 2yyx^7 + \{y^4 + 6y^3 - \tfrac{5}{2}(y^2 + yy)\}x^8 + 12y^2yx^9\\
&\quad + \{2y^6 + 8y^5 + 18y^4 + 4y^3y + 6(y^2y + yyy) + 2y^2y^2 - 16(y^3 + y^2y)\}x^{10}\\
&\quad + \{8y^4y + 40y^3y + 14y^2y^2 + 4y^2yy - 16(2y^2y + yyy)\}x^{11}\\
&\quad + \{y^9 + 6y^8 + 22y^7 + 40y^6 + 55y^5 + 8y^5y + 24y^4y + 4y^4y^2 + 24y^3y^2\\
&\quad + 28(y^3y + y^2yy) + 26(y^2y^2 + y^2yy) + (y^2y^2 + 2y^2yy + yyyy)\\
&\quad - 23(y^4 + y^2y^2) - 12(y^5 + y^4y) - 62(y^4 + y^3y) + \tfrac{31}{3}(y^3 + 3y^2y + yyy)\}x^{12}\\
&\quad + \{20y^6y + 68y^5y + 132y^4y + 4(y^3y + 3y^2yy + yyyy) + 24y^4y^2\\
&\quad + 8(y^4y + y^3yy) + 24(y^3y^2 + y^3yy) + 88y^3y^2 + 16(y^3y^2 + y^2y^2y)\\
&\quad + 14(y^2y^2 + 3y^2yy + yyyy) + 6y^3y^3 + 16y^2y^2y + 4y^4yy\\
&\quad + 16y^3yy - 46(2y^3y + y^2yy) - 124(y^3y + y^2y^2 + y^2yy)\}x^{13} + \ldots.
\end{aligned}
$$

This form may be specialized to $q = 3$ by putting $y_3 = y_4 = 0$.

The series that may be derived from this expression are

$$\sum F_m x^m = -\frac{1}{kT}F(0; T);$$

$$\sum U_m x^m = x\frac{\mathrm{d}}{\mathrm{d}x}\left(-\frac{1}{kT}F(0; T)\right),$$

which is the low temperature expansion for $(1/\epsilon_1)U$;

$$\sum C_m x^m = x\frac{\mathrm{d}}{\mathrm{d}x}x\frac{\mathrm{d}}{\mathrm{d}x}\left(-\frac{1}{kT}F\right),$$

which is the expression for $\epsilon_1^{-2}kT^2C$; and the series expressions for Ψ_0 (equation (7)), $kT\chi$ (equation (8)), and $kT\chi_\perp$ (equation (9)). The coefficients of these series are given in table 3.

Table 3. Coefficients of series expansions of various functions

	$-\frac{1}{kT}F$	$\frac{1}{\epsilon_1}U$	$\frac{kT^2}{\epsilon_1^2}C$	Ψ_0	$kT\chi$	$kT\chi_{\perp}$
x^0	0	0	0	1	0	0
x^4	2	8	32	−3	2	2
x^6	4	24	144	−12	16	16
x^7	4	28	196	−12	16	0
x^8	4	32	256	−36	100	120
x^9	24	216	1944	−108	216	24
x^{10}	16	160	1600	−210	844	844
x^{11}	60	660	7260	−480	1552	400
x^{12}	$172\frac{2}{3}$	2072	24864	−1746	7844	5924
x^{13}	128	1664	21632	−2340	12112	4448
x^{14}	840	11760	164640	From Kihara *et al* (1954)		
x^{15}	1180	17700	265500			
x^{16}	2576	41216	659456			

References

Domb C 1960 *Adv. Phys.* **9** 149–361

Essam J W and Fisher M E 1963 *J. chem. Phys.* **38** 802–12

Fisher M E 1967 *Rep. Prog. Phys.* **30** 615–730

—— 1969 *J. Phys. Soc. Japan Suppl.* **26** 86 (*Proc. IUPAP Conf. Stat. Mech.*)

Fisher M E and Ferdinand A E 1967 *Phys. Rev. Lett.* **19** 169–72

Griffiths R B 1970 *Phys. Rev. Lett.* **24** 715–7

—— 1973 *Phys. Rev.* B **7** 545–51

Kihara T, Midzuno Y and Shizume T 1954 *J. Phys. Soc. Japan* **9** 681–7

Kadanoff L P *et al* 1967 *Rev. mod. Phys.* **39** 395–431

Landau L D 1937 *Phys. Z. Sowjun.* **11** 26 (English translation: 1965 *Collected Papers of L D Landau*, ed ter Haar (London: Gordon and Breach) pp 193–216)

Mittag L and Stephen M J 1971 *J. math. Phys.* **12** 441–50

Potts R B 1952 *Proc. Camb. Phil. Soc.* **48** 106–9

Roozeboom H W B 1913 *Die heterogenen Gleichgewichte von Standpunkte der Phasenlehre* (Viewig and Sohn: Braunschweig) pp 32, 128, 204

Rushbrooke G S 1963 *J. chem. Phys.* **39** 842

Zwanzig R 1963 *J. chem. Phys.* **39** 1714–21